Phys. Status Solidi C **6**, No. S1, S46–S49 (2009) / **DOI** 10.1002/pssc.200881304

physica status solidi c
www.pss-c.com
current topics in solid state physics

Ultrafast coherent vibronic oscillations in regioregular poly(3-alkylthiophene)

Katsuichi Kanemoto*, Mitsuru Sugisaki, Masazumi Fujiwara, Tsutomu Karasawa, and Hideki Hashimoto

CREST/JST and Department of Physics, Osaka City University, 3-3-138 Sugimoto, Sumiyoshi-ku, Osaka 558-8585, Japan

Received 26 August 2008, revised 10 October 2008, accepted 10 October 2008
Published online 9 April 2009

PACS 42.65.Sf, 78.47.jj, 78.66.Qn, 82.53.Kp

* Corresponding author: e-mail kkane@sci.osaka-cu.ac.jp, Phone: +81 6 6605 2550, Fax: +81 6 6605 2522

Ultrafast degenerate four-wave mixing (DFWM) signals of the regioregular (RR) poly(3-hexylthiophene) (P3HT) film have been investigated by the experiments using sub-20 fs pulses generated from a noncollinear optical parametric amplifier (NOPA) system. Strong DFWM signals were observed owing to a large third-order nonlinear susceptibility $\chi^{(3)}$ of the RR-P3HT film. The time profile of the DFWM signals exhibits clear coherent oscillation on a decaying signal. The oscillation turn out to be caused by the C=C stretching mode that gives strong Raman signal. The time profile of the DFWM signal is simulated by a numerical calculation. The result of simulation reveals that decay constants of electronic population and of vibronic oscillation are 200 fs and 210 fs, respectively. This is the first determination of the decay constants for the RR-P3HT film. The obtained result demonstrates that the $\chi^{(3)}$ signal of the RR-P3HT film decays very rapidly.

1 Introduction The magnitude of the third-order nonlinear susceptibility $\chi^{(3)}$ of π-conjugated molecules is known to increase with the number of double bonds or the chain length [1]. One thus expects that conjugated polymers, with quite a few double bonds, exhibit a large value of $\chi^{(3)}$. Hence, conjugated polymers have attracted a great interest as one of promising organic nonlinear optical materials [2]. Among some classes of conjugated polymers, poly(3-alkylthiophene) (P3AT) is one of the most studied polymers owing to its potential applicability as organic semiconducting materials and its good solubility to several familiar solvents that enables the film fabrication by wet processes. Head-to-tail coupled, regioregular (RR) P3AT is particularly noticeable, because it has been demonstrated that the magnitude of $\chi^{(3)}$ in P3AT is enhanced by arranging its alkyl sidechains in a head-to-tailed way [3-5].

Among some characters of $\chi^{(3)}$ reported on RR-P3AT, we focus on $\chi^{(3)}$ (ω; ω, ω, $-\omega$) determined using a degenerate four-wave mixing (DFWM) method. Previously, a large value of $\chi^{(3)}$ (ω; ω, ω, $-\omega$) whose magnitude reaches as much as 10^{-7} esu at the resonance condition was reported for the Langmuir–Blodgett (LB) film of RR-P3AT [6]. This arouses our interest in the dynamics of the very early process of the large $\chi^{(3)}$ (ω; ω, ω, $-\omega$).

In this article, the very early process of $\chi^{(3)}$ (ω; ω, ω, $-\omega$) signals in RR type poly(3-hexylthiophene) (P3HT) (Fig. 1) is addressed by DFWM experiments using sub-20 fs pulses at the resonance condition. The presence of clear coherent vibronic oscillations is demonstrated in the DFWM experiments. The decay constants of the dephasing and of the electronic excited states for RR-P3AT are determined for the first time. We emphasize that this determination would be a first step to investigate the photophysics of the early process after photoexcitation of RR type P3AT.

2 Experimental RR-P3HT used in this study was purchased from Aldrich. The film sample of RR-P3HT was made by spin-casting its chloroform solution onto a quartz substrate. The absorption spectrum was recorded with a

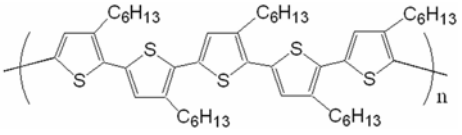

Figure 1 Chemical structure of regio-regular (RR) poly(3-hexylthiophene) (P3HT).

SHIMAZU UV-2400 spectrometer. The Raman spectrum was measured using an Ar^+ laser at 488 nm as a light source under the spectral resolution of < 5 cm^{-1}.

As light source required for ultrafast optical measurements, a noncollinear optical parametric amplifier (NOPA) was used. The details of the NOPA system were previously described [7]. Initially, a femtosecond Ti:sapphire regenerative amplifier (Spectra Physics, Hurricane) was used to generate 100 fs pulses at 800 nm at a 1 kHz repetition rate. Part of the beam from the amplifier (~ 400 μJ) was used for the NOPA system. The pump pulses for the NOPA were obtained by frequency doubling the main fraction of the laser beam in a 400-μm-thick β-BaB_2O_4 (BBO) crystal. The residual of the fundamental laser beam was passed through a delay line for synchronization and then focused onto a 1 mm thick sapphire plate in order to generate white-light continuum pulses. The amplified beam, having ~1 μJ in power, was collimated by a spherical lens and then sent to a pulse compressor. By adjusting the insertion of the Brewster prism, the pulse width was optimized. For the measurement of the DFWM signals, the compressed output beam from the NOPA was divided into three using pellicle membranes with a thickness of 2 μm.

The DFWM measurements were performed for the RR-P3HT film kept under nitrogen gas in order to minimize sample degradation by the laser irradiation. The pulse width was determined by measuring the cross correlations using a 100-μm-thick BBO crystal. The pulse width was optimized down to 19.6 fs at 630 nm, which is near the absorption edge of the sample. As shown in Fig. 2(a), the three pump pulses in the triangular configuration were focused onto the surface of the sample cell. After passing through the sample, the nonlinear signals were spatially selected using an iris of ~1 mm diameter with a photomultiplier tube (Hamamatsu, R636-10). The signal was filtered by ordering of pulse sequences as shown in Fig. 2(b). All measurements were carried out at room temperature.

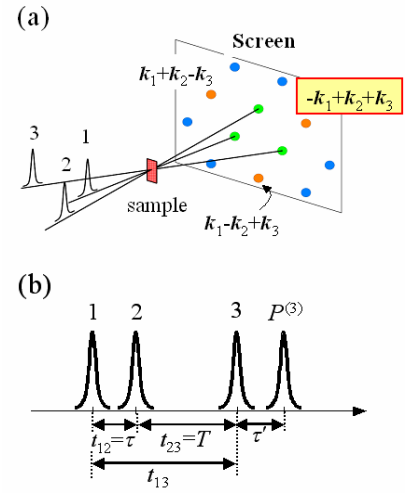

Figure 2 (a) Spatial configuration of the degenerate four-wave mixing (DFWM) experiment. Three consecutive pulses from the noncollinear optical parametric amplifier (NOPA) with wave vectors $\boldsymbol{k}_1$, $\boldsymbol{k}_2$, and $\boldsymbol{k}_3$ are focused in a triangular geometry into the sample. (b) Time ordering of pulse sequences and notations of time intervals. τ and T denote the center-to-center distances between the pulse pairs (1, 2) and (2, 3), respectively. τ' denotes the delay of the signal from pulse 3.

3 Results and discussion The absorption spectrum at room temperature of the RR-P3HT film is shown in Fig. 3(a). The spectrum exhibits three weak peaks around at 2.06, 2.23 and 2.41 eV. The spacing of the peaks, 0.17-0.18 eV, corresponds to the vibrational splitting of the C=C stretching mode. Figure 3(b) shows the Raman spectrum irradiated at 488 nm of RR-P3HT after eliminating back-

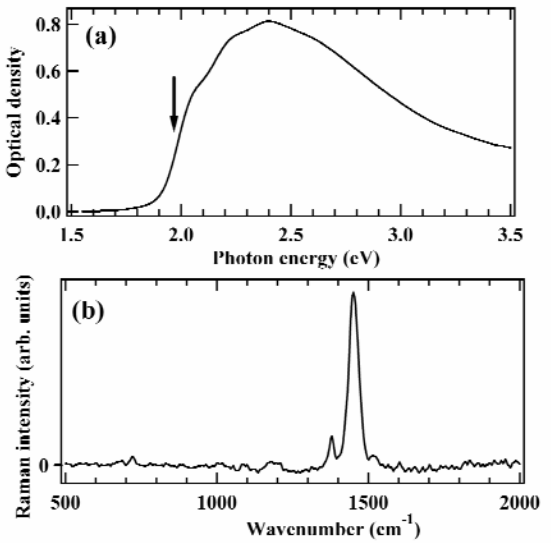

Figure 3 (a) Absorption spectrum at room temperature of RR-P3HT film. (b) Raman spectrum of the RR-P3HT film irradiated at 488 nm (the spectral resolution < 5 cm^{-1}). The background signal from photoluminescence was eliminated.

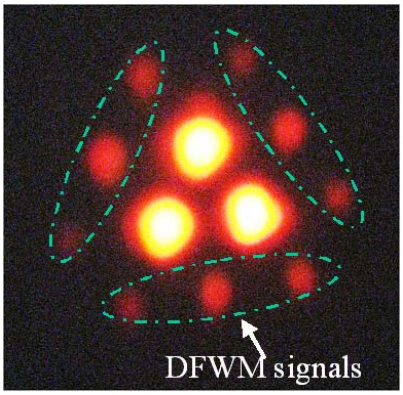

Figure 4 Photoimage of the output signal of the DFWM experiment for the RR-P3HT film. The third-order optical responses or DFWM signals are marked by the dotted ovals. The three intense spots in the middle are the pump beams.

ground signals from photoluminescence. The Raman spectrum is dominated by strong signals around 1450 cm^{-1} that are assigned to the C=C stretching mode [8, 9] and consistent with the spacing observed in the absorption spectrum.

The photograph in Fig. 4 shows the DFWM signal taken just behind the RR-P3HT film. The time delay among all pump beams was set to zero ($t_{12} = t_{13} = 0$, see Fig. 2). In addition to the pump-beam spots with a triangle shape at the center, the nonlinear signals are clearly observed surrounding them. The spots marked by the dotted ovals are the DFWM signals. These signals that can be clearly observed by eye indicate that the P3HT film is attractive as nonlinear optical materials and suitable for nonlinear spectroscopy.

Figure 5 shows the DFWM signal of the P3HT film as a function of the population period t_{13}. The temporal separation between pulses 1 and 2 (t_{12}) was set to zero; i.e., obtained is the transient grating signal. An intense signal is observed at $t_{13} = 0$. A coherent oscillation with a period of about 25 fs is superimposed on a gradually decaying signal. This ultrafast oscillation is a first observation for polythiophene derivatives. The clear decay of the oscillation is identified after subtracting the contribution of the gradually decaying signal, as shown in the inset in Fig. 5. Figure 6 shows the Fourier spectrum of the oscillation signals presented in the inset in Fig. 5. The Fourier spectrum is dominated by strong signals at around 1450 cm^{-1} and close to the Raman spectrum shown in Fig 3(b). Therefore it is concluded that the coherent oscillation observed in the DFWM experiment stems from the molecular vibration of the C=C stretching mode.

We now attempt to fit the time profile of the DFWM signal by a numerical calculation. In the homodyne detection scheme, the DFWM signal S_D is given by the time-integrated signal along the $\boldsymbol{k}$ direction,

$$S_D(\tau,T) = \int_0^\infty dt \left| P^{(3)}(\boldsymbol{k},t) \right|^2 \qquad (1)$$

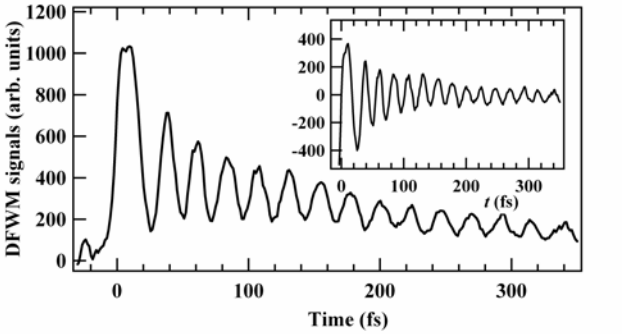

Figure 5 Transient grating signal for the RR-P3HT film as a function of the population time t_{13}. The temporal separation of pulses 1 and 2 (t_{12}) was set to zero. The vibronic coherent oscillation is obtained by subtracting the gradually varying background due to the electronic relaxation. The residual signal is shown in the inset.

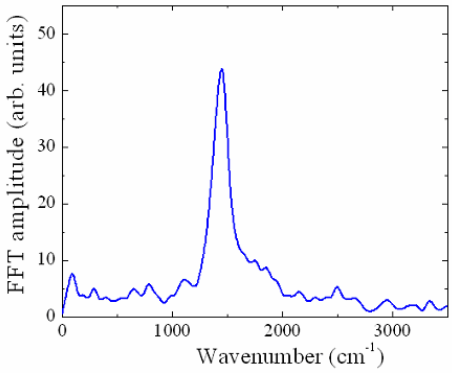

Figure 6 Fourier transform spectrum for the coherent oscillations shown in the inset in Fig. 5.

where $P^{(3)}(\boldsymbol{k}, t)$ is the third-order polarization and τ and T are the center-to-center distances between the pulse pairs (1, 2) and (2, 3), see Fig. 2. Invoking the rotating wave approximation, Eq. (1) can be simplified under the impulsive limit as [10].

$$S_D(\tau,T) \approx \left| R(\tau,T,\tau) \right|^2, \qquad (2)$$

where $R(\tau, T, \tau)$ is the total response function.
We here assume a simple two-level system consisting of the ground state S_0 and the photo-excited state S_1. The total response function is then obtained by [10]

$$R = R_1 + R_2 \quad , \qquad (3)$$

with

$$\begin{aligned} R_1 &= \left|\mu_{10}\right|^2 \exp[-g^*(\tau) + g^*(T) - g(\tau') \\ &- g^*(\tau+T) - g^*(T+\tau') + g^*(\tau+T+\tau')], \\ R_2 &= \left|\mu_{10}\right|^2 n_1 \exp[-g^*(\tau) + g(T) - g^*(\tau') \\ &- g^*(\tau+T) - g(T+\tau') + g^*(\tau+T+\tau')], \end{aligned} \qquad (4)$$

where μ_{10} is the transition dipole interaction between S_1 and S_0. n_1 represents the relaxation rate of population from S_1 to S_0. Double-sided Feynman diagrams for the R_1 and R_2 processes are shown in Fig. 7. $g(t)$ is the line broadening

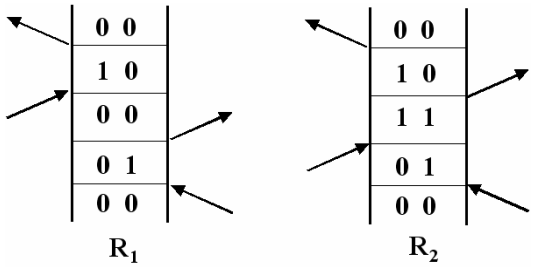

Figure 7 Double-sided Feynman diagrams for the R_1 and R_2 processes. The symbols 0 and 1 indicate the S_0 and S_1 states, respectively.

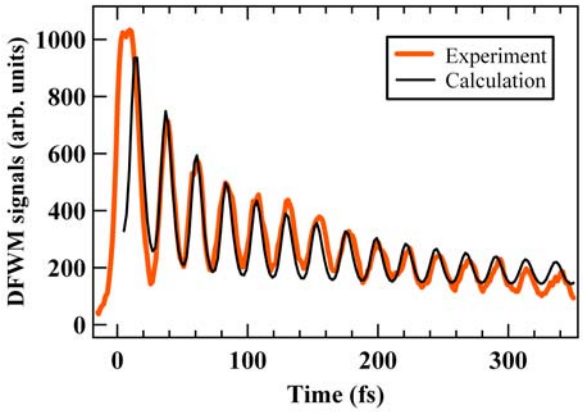

Figure 8 Fitting result for the transient grating signals as a function of the temporal separation of pulses 1 and 3 (t_{13}). The thick and thin solid curves indicate the results of experiment and calculation, respectively.

function that indicates the time evolution of the transition frequency correlation and is calculated from the spectral density [10].

Actual calculation to simulate the time profile shown in Fig. 5 was carried out by assuming a single component for population relaxation n_1 and treating a single mode for oscillation. Also we used the conditions that $\tau \approx \tau'$, and the value of τ less than 5 fs was numerically integrated to incorporate the effect of the finite pulse width. The result of the calculation is shown in Fig. 8. It indicates that our calculation represents well the time profile of the DFWM signal for the P3HT film. In the calculation, we used 200 fs for the time constant of the population decay. This value is much smaller than the time constant of photoluminescence (PL) decay (~several hundreds of picoseconds [11, 12]). This suggests that species generated after some relaxation processes are responsible for PL. Also, the best agreement between the theoretical calculation and experimental observation was seen by 1452 cm^{-1} for the center mode of oscillation and by 25cm^{-1} for the Lorentzian full width at half maximum (FWHM). The latter parameter determines the time constant for the dephasing of vibronic oscillation as 210 fs. The decay process of transient grating signals of RR-P3HT was previously investigated by experiments using 120 fs pulses and it was reported that the decay constant of population would be less than 2 ps [4]. Our result is consistent with the previous report and determines the decay constant of RR-P3HT for the first time. This determination would be a first step to investigate the physics of the early process in the coherent state of RR P3AT. Further study is under progress.

4 Conclusions The DFWM experiments for the film of head-to-tail coupled RR-P3HT were performed using sub-20fs pulses generated from the NOPA system. Strong transient grating signals, which can be observed by eye, were identified. It indicates that the RR-P3HT film is attractive as nonlinear optical materials. In the time profile of the transient grating signal, clear coherent oscillation was observed on a decaying signal. The oscillation turned out to be caused by the C=C stretching mode that gave strong Raman signal. The time profile of the transient grating signal was simulated by a numerical calculation. The theoretical simulation revealed that decay constants of electronic population and of vibronic oscillation are 200 fs and 210 fs, respectively. This is the first determination of the decay constants for the RR-P3HT film.

References

[1] I. D. W. Samuel, I. Ledoux, C. Dhenaut, J. Zyss, H. H. Fox, R. R. Schrock, and R. J. Silbey, Science **265**, 1070 (1994).
[2] J. L. Brédas, C. Adant, P. Tackx, and A. Persoons, Chem. Rev. **94**, 243 (1994).
[3] T. Bjørnholm, D. R. Greve, T. Geisler, J. C. Petersen, M. Jayaraman, and R. D. McCullough, Adv. Mater. **8**, 920 (1996).
[4] H. Kawahara, Y. Ueno, N. Abe, S. Kishino, K. Ema, M. Rikukawa, Y. Tabuchi, and N. Ogata, Opt. Rev. **4**, 188 (1997).
[5] H. Kishida, K. Hirota, T. Wakabayashi, H. Okamoto, H. Kokubo, and T. Yamamoto, Appl. Phys. Lett. **87**, 121902, (2005).
[6] S. Kishino, Y. Ueno, K. Ochiai, M. Rikukawa, K. Sanui, T. Kobayashi, H. Kunigita, and K. Ema, Phys. Rev. B **58**, R13430 (1998).
[7] M. Sugisaki, K. Yanagi, R. J. Cogdell, and H. Hashimoto, Phys. Rev. B **75**, 155110 (2007).
[8] G. Louarn, M. Trznadel, J. P. Buisson, J. Laska, A. Pron, M. Lapkowski, and S. Lefrant, J. Phys. Chem. **100**, 12532 (1996).
[9] P. J. Brown, D. S. Thomas, A. Köhler, J. S. Wilson, J. S. Kim, C. M. Ramsdale, H. Sirringhaus, and R. H. Friend, Phys. Rev. B **67**, 064203 (2003).
[10] S. Mukamel, Principles of Nonlinear Optical Spectroscopy (Oxford University Press, New York, 1995).
[11] T. Kobayashi, J. Hamazaki, H. Kunugita, and K. Ema, Phys. Rev. B **67**, 205214 (2003).
[12] K. Kanemoto, I. Akai, and T. Karasawa, unpublished result.